European Heart Journal
doi:10.1093/eurheartj/ehu281

2014 ESC Guidelines on the diagnosis and treatment of aortic diseases - web addenda

Document covering acute and chronic aortic diseases of the thoracic and abdominal aorta of the adult

The Task Force for the Diagnosis and Treatment of Aortic Diseases of the European Society of Cardiology (ESC)

Authors/Task Force members: Raimund Erbel* (Chairperson) (Germany), Victor Aboyans* (Chairperson) (France), Catherine Boileau (France), Eduardo Bossone (Italy), Roberto Di Bartolomeo (Italy), Holger Eggebrecht (Germany), Arturo Evangelista (Spain), Volkmar Falk (Switzerland), Herbert Frank (Austria), Oliver Gaemperli (Switzerland), Martin Grabenwöger (Austria), Axel Haverich (Germany), Bernard Iung (France), Athanasios John Manolis (Greece), Folkert Meijboom (Netherlands), Christoph A. Nienaber (Germany), Marco Roffi (Switzerland), Hervé Rousseau (France), Udo Sechtem (Germany), Per Anton Sirnes (Norway), Regula S. von Allmen (Switzerland), Christiaan J.M. Vrints (Belgium)

ESC Committee for Practice Guidelines (CPG): Jose Luis Zamorano (Chairperson) (Spain), Stephan Achenbach (Germany), Helmut Baumgartner (Germany), Jeroen J. Bax (Netherlands), Héctor Bueno (Spain), Veronica Dean (France), Christi Deaton (UK), Çetin Erol (Turkey), Robert Fagard (Belgium), Roberto Ferrari (Italy), David Hasdai (Israel), Arno Hoes (The Netherlands), Paulus Kirchhof (Germany/UK), Juhani Knuuti (Finland), Philippe Kolh (Belgium), Patrizio Lancellotti (Belgium), Ales Linhart (Czech Republic), Petros Nihoyannopoulos (UK),

* Corresponding authors: Raimund Erbel, Department of Cardiology, West-German Heart Centre Essen, University Duisburg-Essen, Hufelandstrasse 55, DE-45122 Essen, Germany. Tel: +49 201 723 4801; Fax: +49 201 723 5401; Email: erbel@uk-essen.de.

Victor Aboyans, Department of Cardiology, CHRU Dupuytren Limoges, 2 Avenue Martin Luther King, 87042 Limoges, France. Tel: +33 5 55 05 63 10; Fax: +33 5 55 05 63 84; Email: vaboyans@live.fr

Other ESC entities having participated in the development of this document:

ESC Associations: Acute Cardiovascular Care Association (ACCA), European Association of Cardiovascular Imaging (EACVI), European Association of Percutaneous Cardiovascular Interventions (EAPCI).

ESC Councils: Council for Cardiology Practice (CCP).

ESC Working Groups: Cardiovascular Magnetic Resonance, Cardiovascular Surgery, Grown-up Congenital Heart Disease, Hypertension and the Heart, Nuclear Cardiology and Cardiac Computed Tomography, Peripheral Circulation, Valvular Heart Disease.

National Cardiac Societies document reviewers: listed in the Appendix.

Massimo F. Piepoli (Italy), Piotr Ponikowski (Poland), Per Anton Sirnes (Norway), Juan Luis Tamargo (Spain), Michal Tendera (Poland), Adam Torbicki (Poland), William Wijns (Belgium), Stephan Windecker (Switzerland).

Document reviewers: Petros Nihoyannopoulos (CPG Review Coordinator) (UK), Michal Tendera (CPG Review Coordinator) (Poland), Martin Czerny (Switzerland), John Deanfield (UK), Carlo Di Mario (UK), Mauro Pepi (Italy), Maria Jesus Salvador Taboada (Spain), Marc R. van Sambeek (The Netherlands), Charalambos Vlachopoulos (Greece), Jose Luis Zamorano (Spain).

The disclosure forms provided by the authors and reviewers are available on the ESC website www.escardio.org/guidelines

Keywords Guidelines • Aortic diseases • Aortic aneurysm • Acute aortic syndrome • Aortic dissection • Intramural haematoma • Penetrating aortic ulcer • Traumatic aortic injury • Abdominal aortic aneurysm • Endovascular therapy • Vascular surgery • Congenital aortic diseases • Genetic aortic diseases • Thromboembolic aortic diseases • Aortitis • Aortic tumors

List of Web Figures and Tables

Web addenda . . . 3
- Section 4.3 Imaging: Web Table 1 . . . 3
- Sections 4.3 Imaging, to 4.3.2.1, Transthoracic echocardiography: Web Figure 1 . . . 6
- Sections 4.3 Imaging, to 4.3.2.2, Transoesophageal echocardiography: Web Figure 2 . . . 7
- Sections 4.3 Imaging, to 4.3.2.3, Abdominal ultrasound: Web Figure 3 . . . 7
- Sections 4.3 Imaging, to 4.3.5, Magnetic resonance imaging: Web Figure 4 . . . 8
- Section 4.3.6 Aortography: Web Figure 5 . . . 8
- Section 4.3.6 Aortography: Web Figure 6 . . . 9
- Section 4.3.7 Intravascular ultrasound: Web Figure 7 . . . 10
- Section 4.3.7 Intravascular ultrasound: Web Figure 8 . . . 10
- Section 5.3.1 Ascending aorta: Web Figure 9 . . . 11
- Section 5.3.2 Aortic arch: Web Figure 10 . . . 12
- Section 5.3.2 Aortic arch: Web Figure 11 . . . 13
- Sections 5.3.3 Descending aorta, and 5.3.4, Thoracoabdominal aorta: Web Figure 12 . . . 13
- Section 5.3.4 Thoracoabdominal aorta: Web Figure 13 . . . 14
- Section 6.4.3 Natural history, morphological changes, and complications: Web Figure 14 . . . 14
- Section 7.2.4.2 Diagnostic imaging: Web Figure 15 . . . 15
- Section 7.2.5.3 Follow-up of small abdominal aortic aneurysm: Web Table 2 . . . 16
- Section 9.1.2 Diagnosis: Web Table 3 . . . 16
- Section 10.2 Treatment: Web Table 4 . . . 17

Web addenda

Section 4.3 Imaging: Web Table 1

Web Table 1 Measurement of 'normal' aortic diameter with various imaging techniques*

Authors/year (reference)	Sample size (*n*)	Age range (years)	Imaging modality	Anatomical landmark of the aorta	Absolute diameters (mm)	Indexed values (mm/m^2)
Computed tomography						
Aronberg *et al.*, 1984[29]	102 (retrospective study, subjects without CV disease)	21–61	Chest CT	Ascending aorta (caudal to the aortic arch)	35	N/A
				Descending thoracic aorta (caudal to the aortic arch)	26	N/A
Fleischmann *et al.*, 2001[30]	77 (prospective study, healthy subjects)	19–67	Abdominal helical CT angiogram	Abdominal aorta (portion superior to coeliac trunk)	18 ± 2 / 19 ± 2 (females / males)	N/A
				Abdominal aorta (between coeliac trunk and superior mesenteric artery)	17 ± 2 / 19 ± 2 (females / males)	N/A
				Abdominal aorta (between superior mesenteric artery and first renal artery)	16 ± 2 / 18 ± 2 (females / males)	N/A
				Abdominal aorta (proximal infrarenal segment)	13 ± 2 / 15 ± 2 (females / males)	N/A
				Abdominal aorta (distal infrarenal segment)	13 ± 1 / 15 ± 1 (females / males)	N/A
				Abdominal aorta (denotes iliac arteries)	8 ± 1 / 10 ± 1 (females / males)	N/A
Hager *et al.*, 2002[31]	70 (prospective study, healthy subjects)	17–89	Helical CT with contrast	Aortic valve sinus	29 ± 4 / 30 ± 5 (females / males)	N/A
				Ascending aorta (caudal to the aortic arch)	31 ± 4	N/A
				Descending thoracic aorta (caudal to the aortic arch)	25 ± 4	N/A
Svensson *et al.*, 2002[32]	43 (marfan syndrome subjects / 21 with aortic dissection)	NA	Chest-CT	Ascending aorta	40–44: *n* = 1 (5%) 45–49: *n* = 2 (10%) 50–54: *n* = 6 (28%) >55: *n* = 12 (57%)	N/A
Svensson *et al.*, 2003[33]	40 (subjects with Aortic dissection)	17–80	CT, MRI, TTE, TOE	Ascending aorta	Mean 60 ± 15 < 50: *n* = 5 (13%) 50–55: *n* = 9 (23%) 56–60: *n* = 12 (30%) 61–70: *n* = 8 (20%) >70: *n* = 6 (14%)	N/A
Davies *et al.*, 2006[34]	410 (retrospective study)	9–93	CT, MRI, TTE, TOE, angiography	Thoracic aorta	Mean 52, Range 35-110 35–44: *n* = 129 (32%) 45–54: *n* = 155 (38%) 55–64: *n* = 68 (17%) 65–74: *n* = 32 (8%) ≥75: *n* = 26 (5%)	Mean 28, Range 14-101 <20.0: *n* = 58 (14%) 20.0–27.4: *n* = 195 (48%) 27.5–34.9: *n* = 88 (21%) 35.0–42.4: *n* = 47 (12%) 42.5–49.9: *n* = 13 (3%) ≥50.0: *n* = 9 (2%)
Kaplan *et al.*, 2007[35]	624 (consecutive patients)	24–87	MSCT with contrast	Ascending aorta (pulmonary artery level)	34 ± 5	N/A
Lin *et al.*, 2008[36]	103 (consecutive healthy patients)	51 ± 14	MSCT (end diastolic)	Aortic root (short axis)	29 ± 2 / 32 ± 3 (females / males)	N/A
				Ascending aorta (pulmonary artery level)	28 ± 4 / 28 ± 3 (females / males)	N/A
				Descending thoracic aorta (pulmonary artery level)	20 ± 2 / 22 ± 2 (females / males)	N/A
Allison *et al.*, 2008[37]	504 (consecutive patients: self-referred vs. referred by personal physician)	25–87	EBCT	Abdominal aorta (just inferior to superior mesenteric artery)	19 ± 3 / 23 ± 3 (females / males)	N/A
				Abdominal aorta (midpoint between SMA and aortic bifurcation)	18 ± 3 / 21 ± 3 (females / males)	N/A
				Abdominal aorta (just superior to aortic bifurcation)	17 ± 2 / 20 ± 2 (females / males)	N/A

Authors/year (reference)	Sample size (*n*)	Age range (years)	Imaging modality	Anatomical landmark of the aorta	Absolute diameters (mm)	Indexed values (mm/m²)
Mao *et al.*, 2008[38]	1442 (consecutive healthy patients)	55 ± 11	MSCT / EBCT (end systolic)	Ascending aorta (pulmonary artery level)	31 ± 4 / 34 ± 4 (females / males)	N/A
Wolak *et al.*, 2008[39]	2952 (consecutive patients free of known CHD)	26–75	EBCT diastole	Ascending aorta (pulmonary artery level)	32 ± 4 / 34 ± 4 (females / males)	N/A
				Descending thoracic aorta (pulmonary artery level)	23 ± 3 / 26 ± 3 (females / males)	N/A
Kälsch *et al.*, 2010[23]	4129 (population-based study [Heinz Nixdorf Recall])	45–75	EBCT Non-contrast, diastole	Ascending aorta (pulmonary artery level)	35 ± 4 / 37 ± 4 (females / males)	19.3 ± 2 / 18.2 ± 2 (females / males)
				Descending thoracic aorta (pulmonary artery level)	25 ± 3 / 28 ± 3 (females / males)	13.9 ± 2 / 14.2 ± 2 (females / males)
Laughlin *et al.*, 2011[40]	1926 (population-based study [MESA])	45–84	MSCT non-contrast	Infrarenal abdominal aorta (5 cm proximal to aortic bifurcation)	19 ± 3	N/A
Rogers *et al.*, 2013[24]	3431 (participants in Framingham Heart Study)	28–62	MSCT Non-contrast *Early diastole*	Ascending aorta (pulmonary artery level)	32 ± 4 / 34 ± 4 (females / males)	N/A
				Descending thoracic aorta (pulmonary artery level)	23 ± 3 / 26 ± 3 (females / males)	N/A
				Infrarenal abdominal aorta (one slice level 5 cm above the aorto-iliac bifurcation)	17 ± 2 / 19 ± 3 (females / males)	N/A
				Lower abdominal aorta (1 slice level above the bifurcation of the abdominal aorta into the common iliac arteries)	16 ± 2 / 19 ± 3 (females / males)	N/A
Magnetic resonance imaging						
Burman *et al.*, 2008[41]	120 (healthy volunteers)	20–80	Diastole	Aortic root (cusp–cusp dimension in sinus planes [average of 3])	31 ± 3 / 35 ± 4 (females / males)	18 ± 2 / 18 ± 2 (females / males)
				Aortic root (cusp–commissure dimension in sinus planes [average of 3])	28 ± 3 / 32 ± 4 (females / males)	17 ± 2 / 16 ± 2 (females / males)
				Aortic root (aortic annulus dimension in sagittal LVOT plane)	20 ± 2 / 22 ± 2 (females / males)	N/A
				Aortic root (aortic sinus dimension in sagittal LVOT plane)	29 ± 3 / 32 ± 4 (females / males)	17 ± 2 / 16 ± 2 (females / males)
				Aortic root (sinotubular junction dimension in sagittal LVOT plane)	24 ± 3 / 25 ± 4 (females / males)	N/A
Wanhainen *et al.*, 2008[42]	231 (prospective population-based study)	70 ± 0		Ascending aorta	34 ± 4 / 40 ± 4 (females / males)	N/A
				Descending aorta	28 ± 3 / 32 ± 3 (females / males)	N/A
				Supraceliac aorta	27 ± 3 / 30 ± 3 (females / males)	N/A
				Suprarenal aorta	27 ± 3 / 28 ± 3 (females / males)	N/A
				Largest Infrarenal abdominal aorta	22 ± 3 / 24 ± 5 (females / males)	N/A
				Aortic bifurcation	20 ± 2 / 23 ± 3 (females / males)	N/A
Redheuil *et al.*, 2011[43]	100 (consecutive healthy patients)	20–84	Diastole	Ascending aorta	30 ± 4 / 31 ± 4 (females / males)	N/A
				Proximal descending aorta	22 ± 3 / 24 ± 3 (females / males)	N/A
				Distal descending aorta	20 ± 2 / 21 ± 3 (females / males)	N/A
Turkbey *et al.*, 2013[44]	3 573 (population-based study (MESA))	45–84		Ascending aorta (ascending aorta luminal diameters at the level of the right pulmonary artery)	31 ± 3 / 33 ± 4 (females / males)	N/A

Authors/year (reference)	Sample size (*n*)	Age range (years)	Imaging modality	Anatomical landmark of the aorta	Absolute diameters (mm)	Indexed values (mm/m^2)
Bidimensional transthoracic echocardiography						
Roman *et al.*, 1989[22]	135 (healthy subjects)	20–74		Annulus	23 ± 2 / 26 ± 3 (females / males)	13 ± 1 / 13 ± 1 (females / males)
				Sinuses of Valsalva	30 ± 3 / 34 ± 3 (females / males)	18 ± 2 / 17 ± 2 (females / males)
				Supra-aortic ridge	26 ± 3 / 29 ± 3 (females / males)	15 ± 2 / 15 ± 2 (females / males)
				Proximal ascending aorta	27 ± 4 / 30 ± 4 (females / males)	16 ± 3 / 15 ± 2 (females / males)
Reed *et al.*, 1993[448]	182 (exceed 95th percentile for height)	17–26		Aortic root	27 ± 3 / 32 ± 4 (females / males)	14 ± 2 / 15 ± 2 (females / males)
Aalberts *et al.*, 2008[45]	53 (Marfan patients)	18–59		Aortic root	35 ± 5 / 41 ± 4 (females / males)	N/A
Biaggi *et al.*, 2009[46]	1799 (consecutive subjects with normal cardiac findings)	20–94		Sinuses of Valsalva	31 ± 3 / 34 ± 3 (females / males)	18 ± 2 / 18 ± 2 (females / males)
				Ascending aorta	30 ± 3 / 32 ± 4 (females / males)	18 ± 2 / 18 ± 2 (females / males)
Gautier *et al.*, 2010[47]	353 (normal children)	2–18		Annulus	17 ± 3 / 18 ± 3 (females / males)	N/A
				Sinuses of Valsalva	24 ± 4 / 27 ± 5 (females / males)	N/A
				Sinotubular junction	20 ± 3 / 22 ± 4 (females / males)	N/A
				Ascending aorta	21 ± 4 / 22 ± 4 (females / males)	N/A
Mirea *et al.*, 2013[48]	500 (consecutive subjects)	48 ± 18		Annulus	17–22 / 19–25 (females / males)	12 ± 1 / 12 ± 1 (females / males)
				Sinuses of Valsalva	23–32 / 27–37 (females / males)	17 ± 2 / 17 ± 2 (females / males)
				Sinotubular junction	19–28 / 22–32 (females / males)	15 ± 2 / 14 ± 2 (females / males)
				Ascending aorta	23–33 / 25–36 (females / males)	17 ± 2 / 16 ± 2 (females / males)
				Aortic arch	16–24 / 17–25 (females / males)	12 ± 2 / 11 ± 1 (females / males)
				Angle	N/A	8 ± 1 / 7 ± 1 (females / males)
Muraru *et al.*, 2013[49]	218 (healthy volunteers)	18–80		Aortic root	N/A	17 ± 2 / 17 ± 2 (females / males)
				Sinotubular junction	N/A	16 ± 2 /16 ± 2 (females / males)
				Proximal tubular portion	N/A	17 ± 4 / 17 ± 4 (females / males)
Vriz *et al.*, 2013[26]	422 (healthy volunteers)	16–90		Annulus	19 ± 2 / 21 ± 2 (females / males)	11 ± 1 / 11 ± 1 (females / males)
				Sinuses of Valsalva	28 ± 2 / 32 ± 4 (females / males)	17 ± 2 / 16 ± 2 (females / males)
				Sinotubular junction	23 ± 3 / 26 ± 4 (females / males)	14 ± 1 / 14 ± 2 (females / males)
				Proximal ascending aorta	26 ± 4 / 28 ± 4 (females / males)	16 ± 2 / 15 ± 2 (females / males)
Transoesophageal echocardiography						
Drexler *et al.*, 1990[50]	25 (healthy volunteers)	19–30		Ascending aorta (lateral axes / sagittal axes / cross-sectional area)	N/A	14 ± 3 / 17 ± 3 / 36 ± 10
				Descending aorta (lateral axes / sagittal axes / cross-sectional area)	N/A	± 2 / 13 ± 3 / 19 ± 8

Authors/year (reference)	Sample size (*n*)	Age range (years)	Imaging modality	Anatomical landmark of the aorta	Absolute diameters (mm)	Indexed values (mm/m^2)
X-ray						
Hiratzka *et al.*, 2010[8]				Ascending aorta (pulmonary artery level)	28.6	N/A
				Descending aorta (pulmonary artery level)	25–26 / 24–30 (females / males)	N/A
Abdominal ultrasound						
Lederle *et al.*, 1997[51]	69 905 (veteran subjects from15 medical centres without AAA)	50–79		Infrarenal abdominal aorta	18 ± 3 / 20 ± 3 (females / males)	N/A
Wilmink *et al.*, 1998[52]	11 336 (population-based screening programme)	50–95	Two study groups (Rotterdam / Huntingdon)	Infrarenal abdominal aorta	16 ± 3 / 20 ± 6 vs. 22 ± 5 (females / males)	N/A
Päivänsalo *et al.*, 2000[53]	1007 (hypertensive patients)	40–60		Abdominal aorta (maximal outer diameter)	17 ± 1 / 20 ± 3 (females / males)	N/A
Freiberg *et al.*, 2008[54]	4734 (prospective cohort study)	75 ± 5		Infrarenal abdominal aorta	17 ± 1 / 20 ± 3 (females / males)	N/A
Sconfienza *et al.*, 2013[55]	1200 (consecutive patients without history of AAA)	64–86		Infrarenal abdominal aorta	7–18 / 9–20 (females / males)	N/A
				Abdominal aorta (intermediate)	8–19 / 9–21 (females / males)	N/A
				Abdominal aorta (iliac bifurcation)	7–18 / 8–20 (females / males)	N/A
Necropsy study						
Da Silva *et al.*, 1999[56]	575 (retrospective necropsy study)	19–92	Post-mortem analysis (aortic balloon inflation)	Infrarenal abdominal aorta	16 ± 2 / 18 ± 2 (females / males)	N/A

CHD = coronary heart disease; CT = computed tomography; EBCT = electron beam computed tomography; LVOT = left ventricular outflow tract; MESA = Multi-Ethnic Study of Atherosclerosis; MSCT = multislice computed tomography; NA = not applicable; SMA = superior mesenteric artery. (Provided by H Kälsch, Department of Cardiology, Essen)

Sections 4.3 Imaging, to 4.3.2.1, Transthoracic echocardiography: Web Figure 1

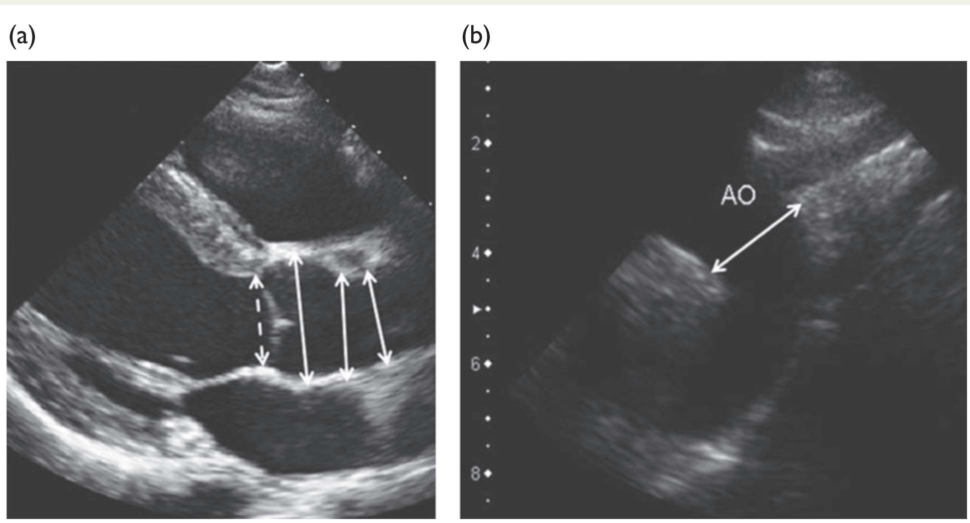

Web Figure 1 Parasternal long-axis and suprasternal imaging of the aorta indicating the points of diameter measurements of the aortic root and aortic arch for transthoracic echocardiography: sinuses of Valsalva; sinotubular junction; ascending aorta; the diameter of the aortic ring (as indicated). AO = aorta.

Sections 4.3 Imaging, to 4.3.2.2, Transoesophageal echocardiography: Web Figure 2

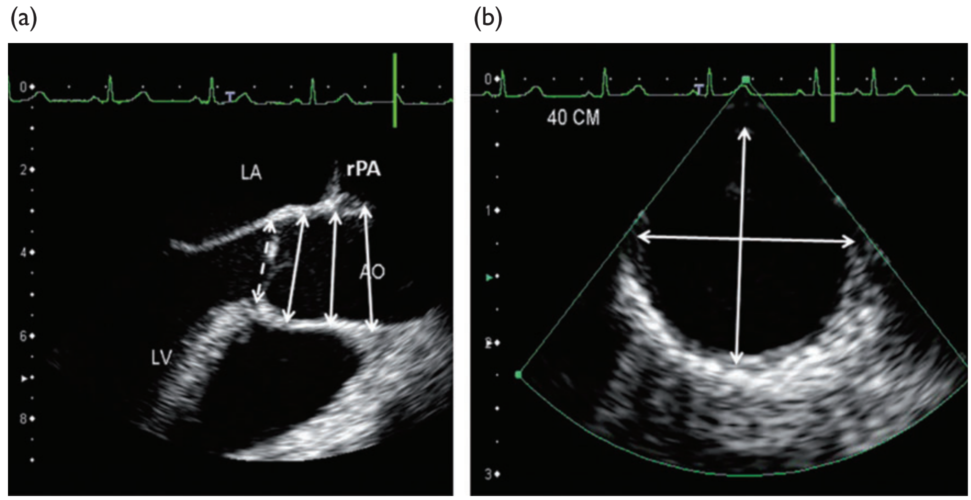

Web Figure 2 Transoesophageal echocardiographic long-axis and cross-sectional image of the ascending and descending aorta, indicating the points of diameter measurements: sinus of Valsalva, beginning of the ascending aorta, ascending aorta at the level of the right pulmonary artery; the diameter of the aortic ring. AO = aorta; LA = left atrium; LV = left ventricle; rPA = right pulmonary artery.

Sections 4.3 Imaging, to 4.3.2.3, Abdominal ultrasound: Web Figure 3

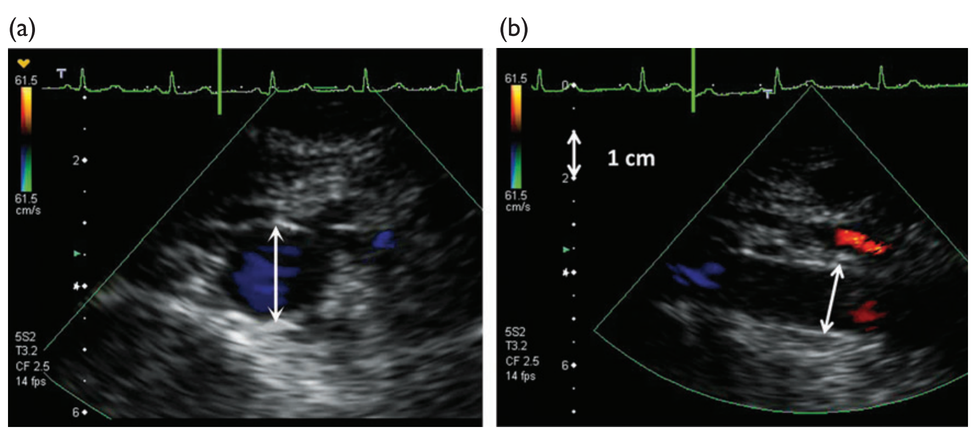

Web Figure 3 Cross-sectional and long-axis imaging of the abdominal aorta indicating the points of diameter measurements.

Sections 4.3 Imaging, to 4.3.5, Magnetic resonance imaging: Web Figure 4

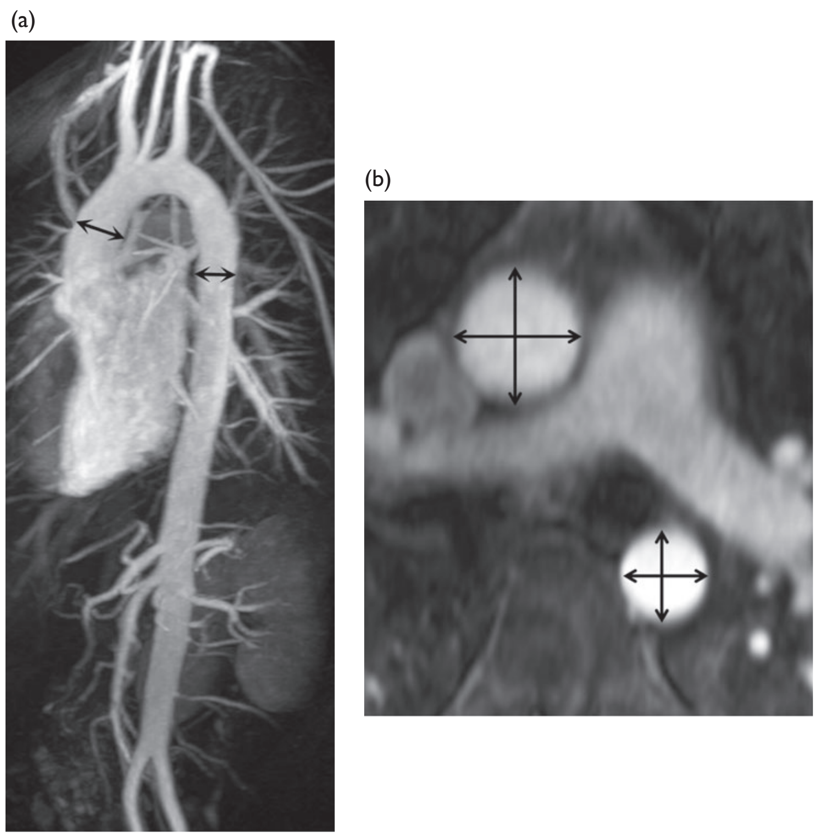

Web Figure 4 Long-axis and cross-sectional imaging of the aorta indicating the points of diameter measurements of the ascending and descending aorta for magnetic resonance imaging. (*Provided by F Nensa, the Institute of Radiology of the University Essen-Duisburg, Germany.)*

Section 4.3.6 Aortography: Web Figure 5

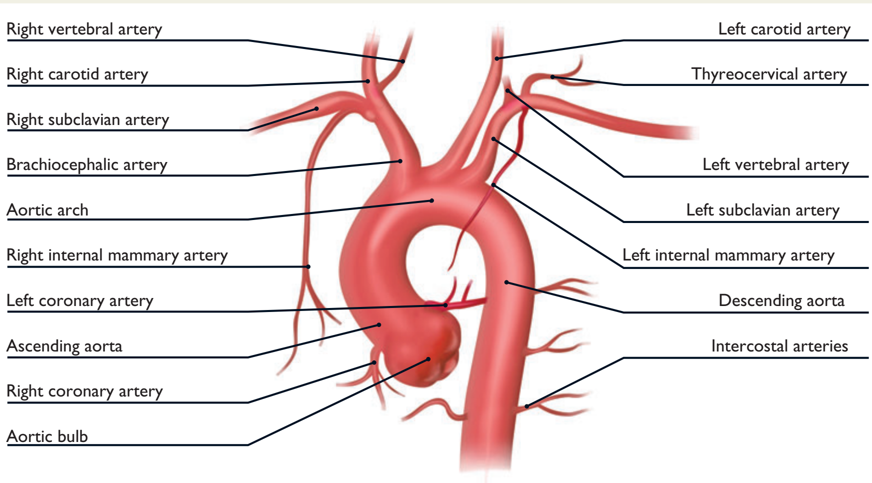

Web Figure 5 Schematic drawing of the aortic arch with the supra-aortic vessels from a left anterior projection. (Modified from Dyer R. Thoracic Aortography. In: *Handbook of Basic Vascular and Interventional Radiology.* New York: Churchill Livingston; 1993).

Section 4.3.6 Aortography: Web Figure 6

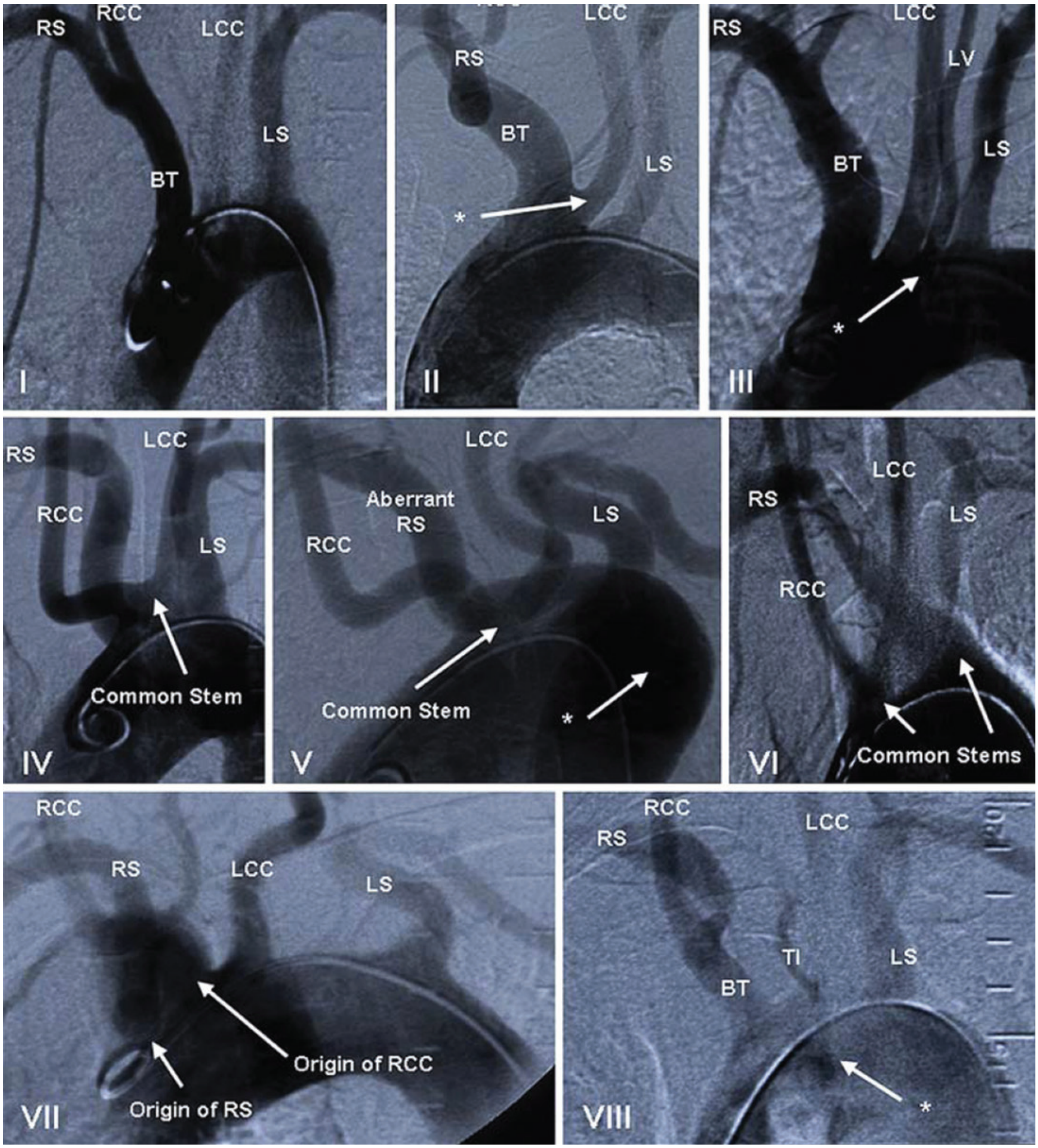

Web Figure 6 Aortic arch anomalies Types I–VIII. Type I is the normal aortic arch found in 64.9–94.3% of cases. The presence of an equine trunk in Type II is not shown as well as the separate origin of the left vertebral artery in Type III (from Natsis KL *et al.*, *Surg Radiol Anat* 2009;31:319–23[91] with permission of Springer Science and Business Media). BT = brachiocephalic trunk (innominate artery); LCC = left common carotid artery; LS = left subclavian artery; LV = left vertebral artery; RCC = right common carotid artery; RS = right subclavian artery; TI = separate thyroid inferior artery.

Section 4.3.7 Intravascular ultrasound: Web Figure 7

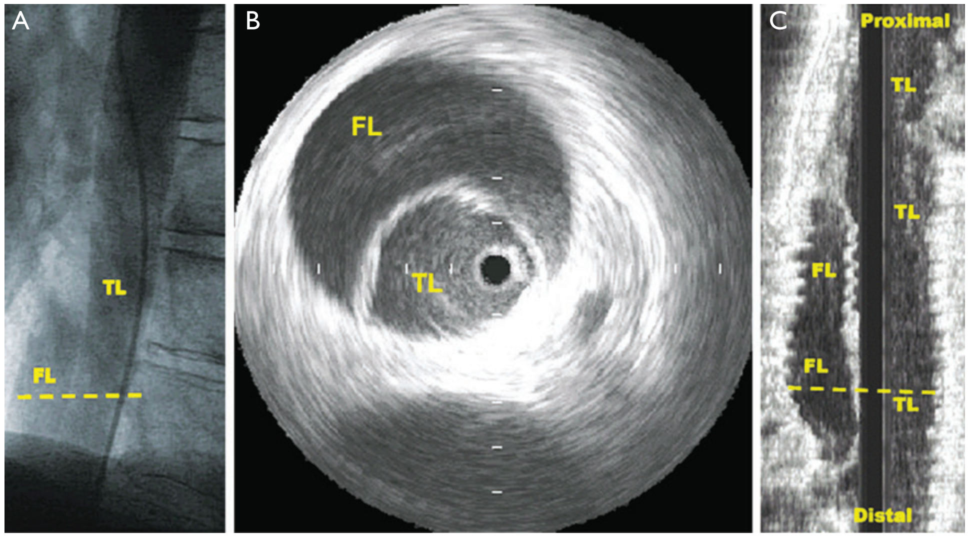

Web Figure 7 Aortic dissection Type B visualized by (A) angiography, (B) cross-sectional intravascular ultrasound with the imaging catheter as a TL, and (C) longitudinal scan after three-dimensional reconstruction using pull-back showing the TL and localized FL. Modified according to Fig. 9.5 in Herzkatheter-Manual, Hrsg. R. Erbel, B Plicht, P. Kahlert, T. Konorza. Dtsch Ärzteverlag 2012, pp277–280 FL = false lumen; TL = true lumen.

Section 4.3.7 Intravascular ultrasound: Web Figure 8

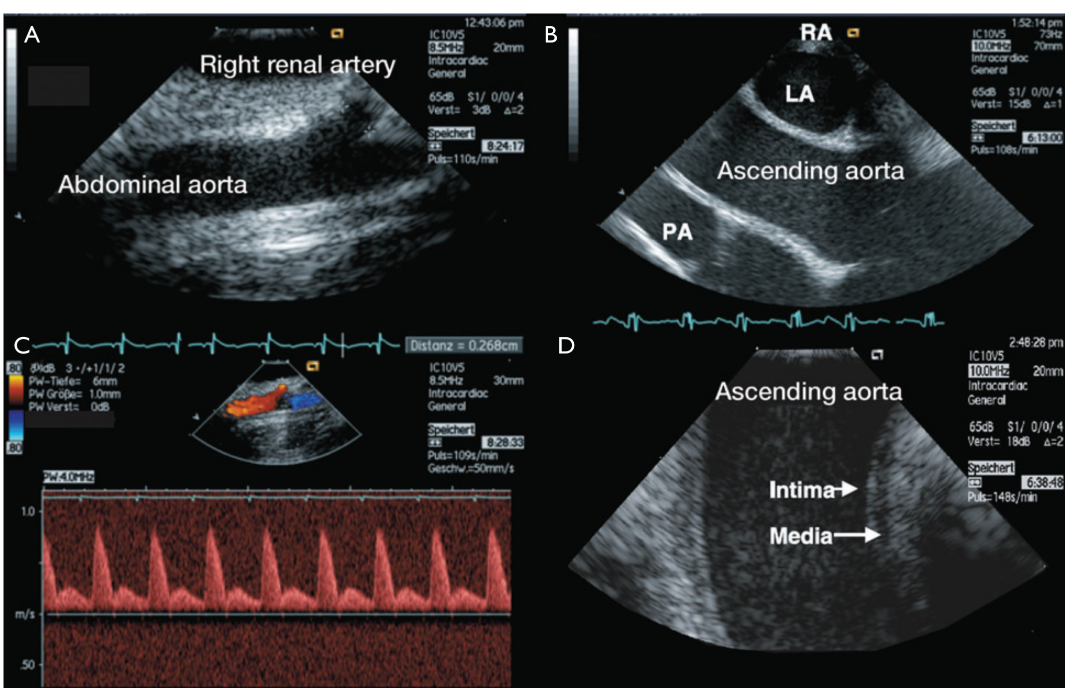

Web Figure 8 Endovascular imaging of the ascending and descending aorta with a phased-array linear intravascular ultrasound 10 MHz transducer showing (A) the high resolution of the system, (A and B) differentiation of intima and media, (C) Doppler flow within the right renal artery as well as the colour Doppler flow, and (D) the abdominal aorta with the origin of the renal artery. Modified according to Fig. 9.7 in Herzkatheter-Manual, Hrsg. R. Erbel, B Plicht, P. Kahlert, T. Konorza. Dtsch Ärzteverlag 2012, pp277–280. AO = aorta; LA = left artery; PA = pulmonary artery; RA = right artery.

Section 5.3.1 Ascending aorta: Web Figure 9

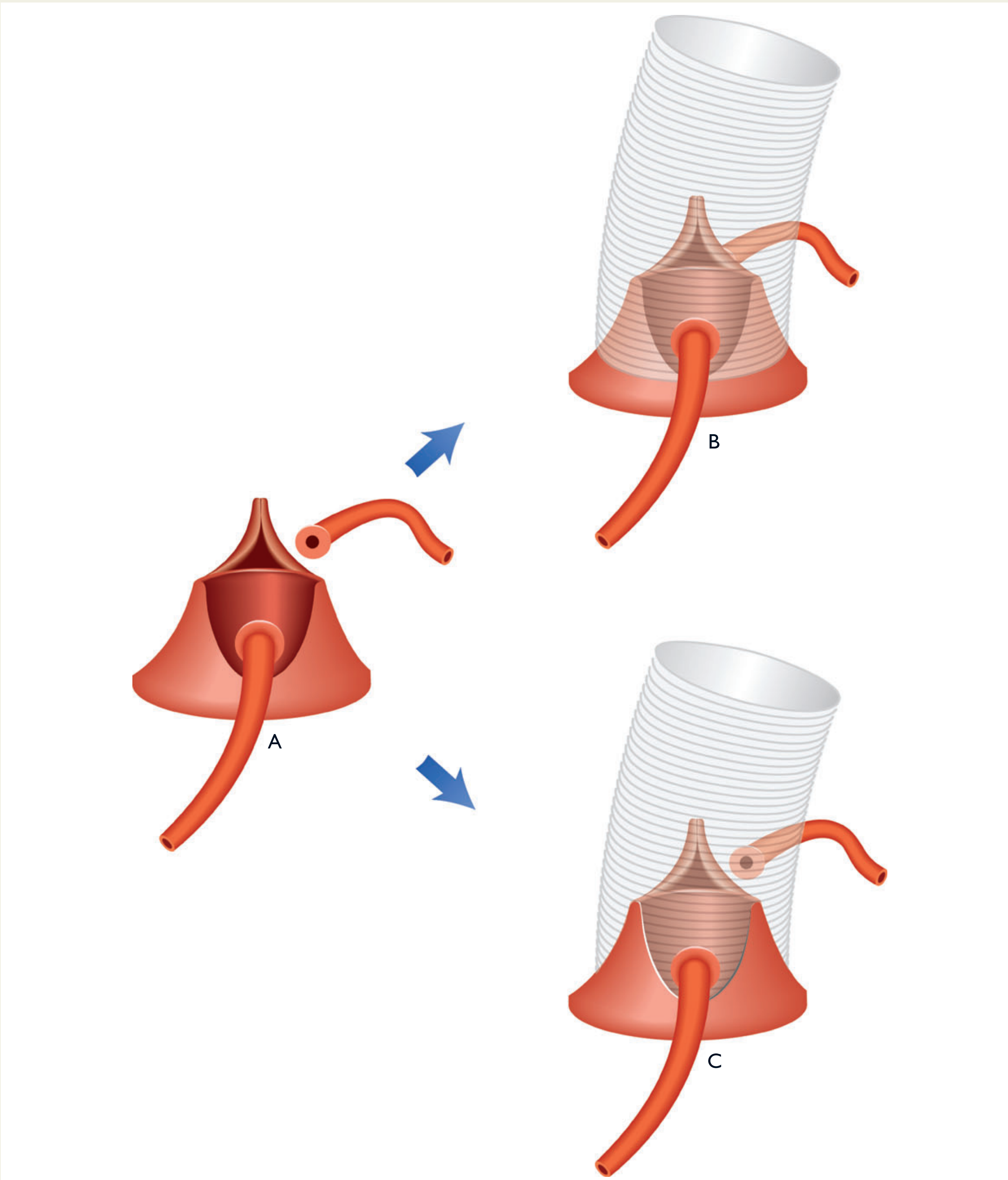

Web Figure 9 (A) Concept of valve-sparing aortic root repair, excision of diseased aorta, and isolation of coronary ostia. (B) Re-implantation technique supporting the aortic annulus with the Dacron prosthesis: David. (C) Remodeling technique without annular support – Yacoub.

Section 5.3.2 Aortic arch: Web Figure 10

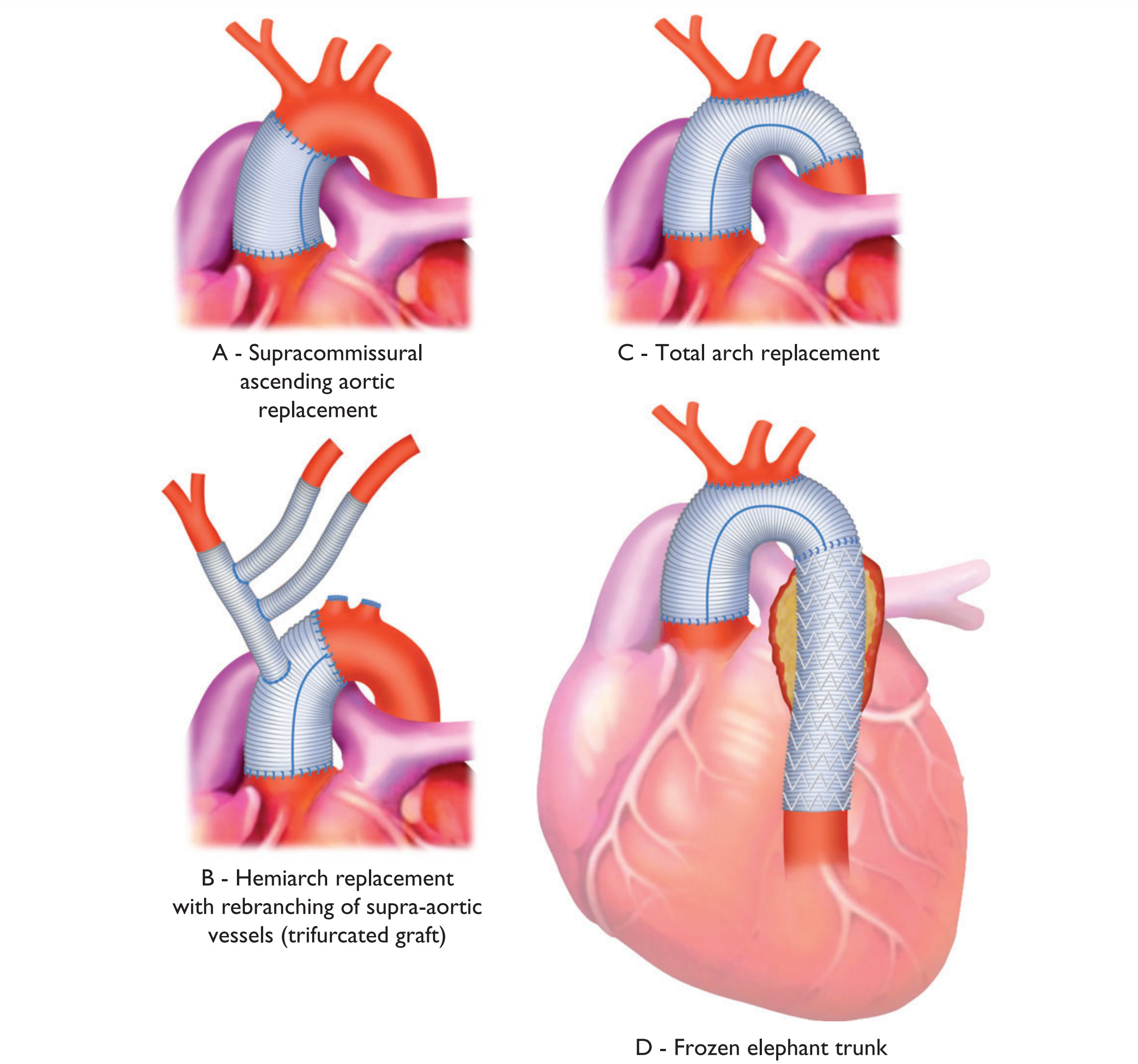

Web Figure 10 (A) Ascending aortic replacement from sinutubular junction to cranial ascending aorta. (B) Hemiarch replacement encompassing the concavity of the aortic arch. (C) Total arch replacement using a trifurcated technique for the supraaortic vessels. (D) Frozen elephant trunk technique including total arch replacement using the island technique.

Section 5.3.2 Aortic arch: Web Figure 11

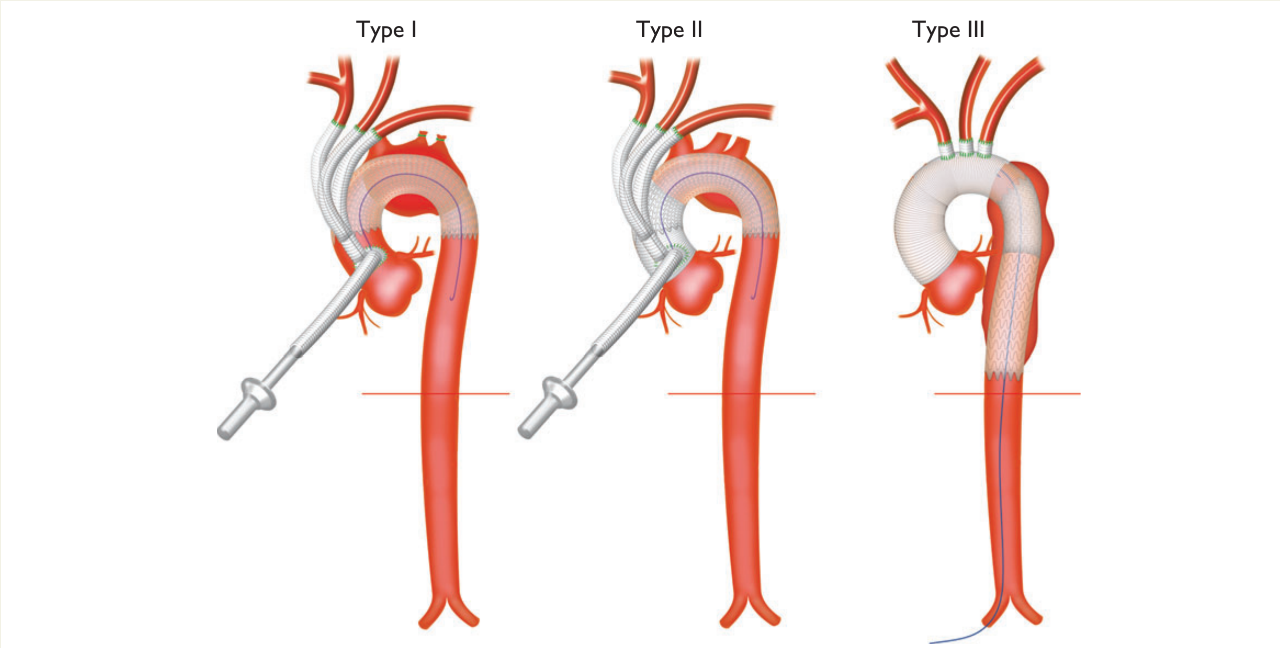

Web Figure 11 Various methods for arch de-branching. Type I: Total arch de-branching and TEVAR for off-pump total arch repair (use of beating heart cardiopulmonary bypass optional). Type II: Total arch de-branching and TEVAR in combination with ascending aortic replacement in patients with proximal disease extension for total thoracic aortic repair Type III: Total arch replacement with conventional elephant trunk technique and distal extension by TEVAR in patients with distal disease extension, for total thoracic aortic repair. TEVAR = thoracic endovascular aortic repair.

Sections 5.3.3 Descending aorta, and 5.3.4, Thoracoabdominal aorta: Web Figure 12

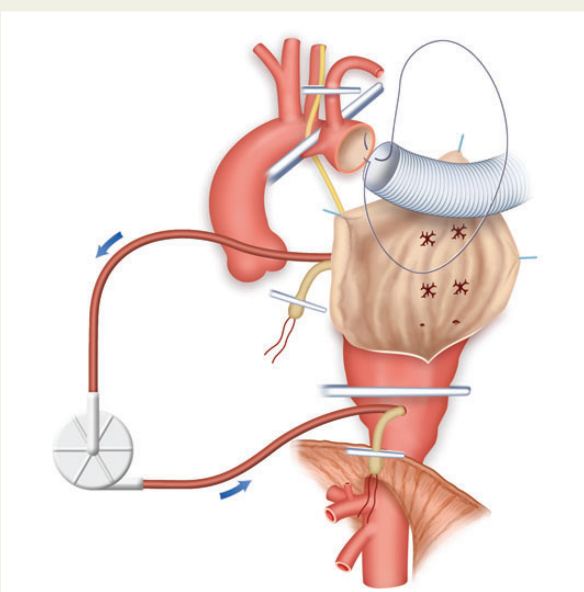

Web Figure 12 Illustration of left heart bypass for thoracic and thoracoabdominal aortic replacement, inflow via left-sided pulmonary veins, and arterial return via any downstream segment.

Section 5.3.4 Thoracoabdominal aorta: Web Figure 13

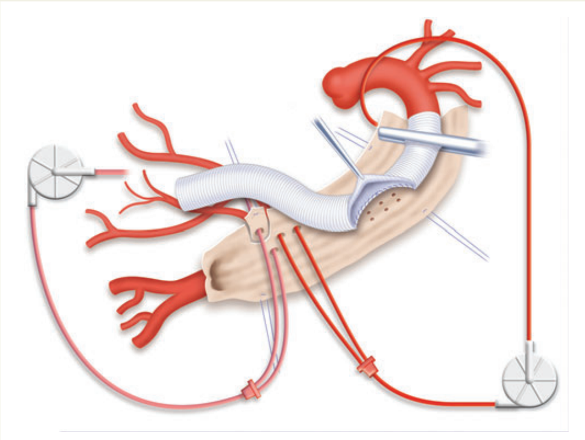

Web Figure 13 Illustration of left heart bypass for thoracic and thoracoabdominal aortic replacement showing selective visceral blood perfusion as well as selective bilateral cold saline perfusion of kidneys.

Section 6.4.3 Natural history, morphological changes, and complications: Web Figure 14

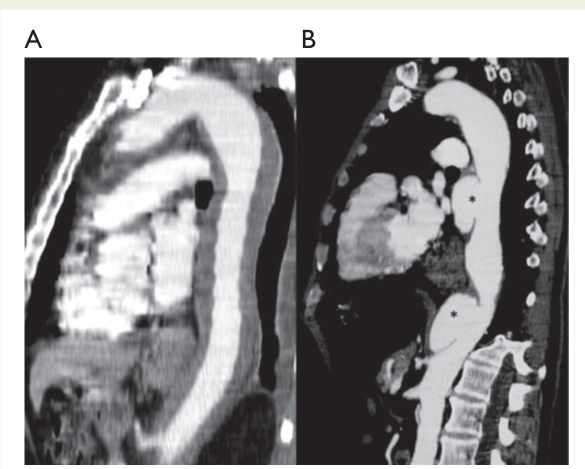

Web Figure 14 Type-B IMH evolving with two localized, ulcer-like projections, 6 months after the acute onset (asterisks).

Section 7.2.4.2 Diagnostic imaging: Web Figure 15

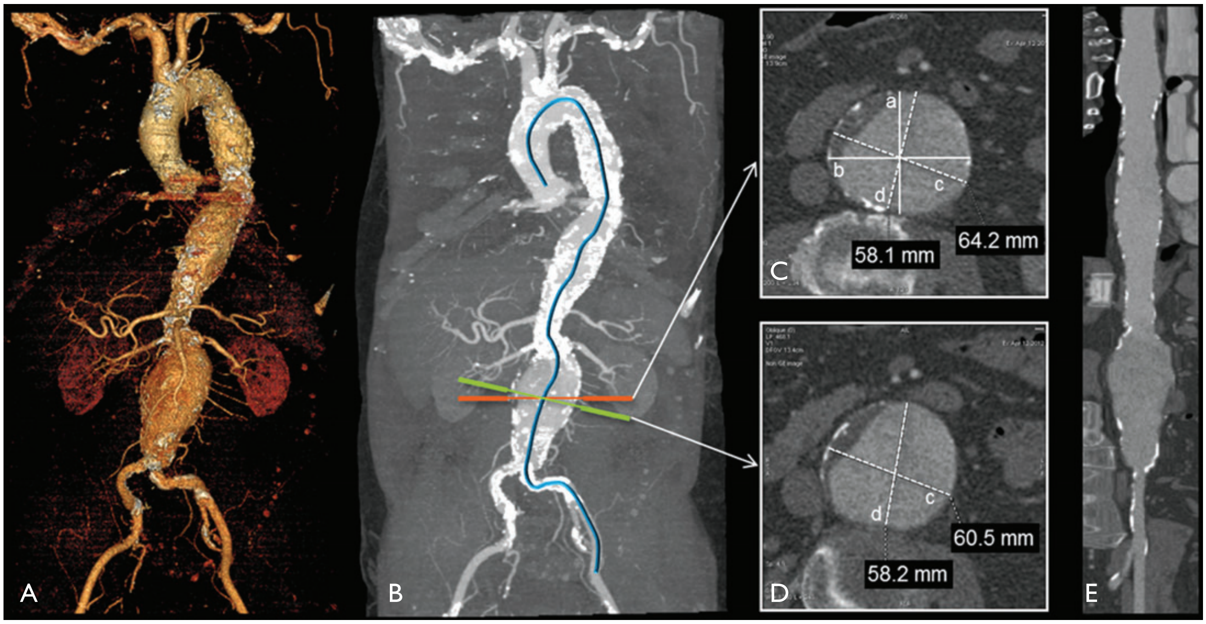

Web Figure 15 CT evaluation of aortic aneurysm. (A) Volume-rendered 3D reconstruction allowing qualitative assessment of the dimensions of the aneurysm and the relationship to side branches (e.g. renal or iliac arteries). It visualizes kinks and tortuosities and is useful for planning interventional procedures. (B) Modern 3D workstations with dedicated software for vascular analysis are recommended and allow the generation of a centreline along tortuous or kinked vessels. (C) Axial cross-section with several accepted methods of measuring the aneurysm diameter: (a) anteroposterior diameter, (b) transverse diameter, (c) maximum short-axis diameter (major axis), and (d) minimal short-axis diameter (minor axis). However, measurement of maximum aneurysm diameter should be performed perpendicular to the vessel centreline (D) rather than on axial cross-sections (particularly in tortuous aneurysms), to avoid over-estimation of maximum diameter, as shown in (C). In this example, maximum diameter on axial cross-section (c in C) is 64.2 mm, while the true maximum diameter is 60.5 mm (c in D). In partially thrombosed aneurysms, it is important to measure up to the outer contour of the aneurysm (C and D). (E) Straight multiplanar reformations are generated automatically upon centreline detection and can provide automatic diameter measurements at any site along the course of the vessel. 3D = three-dimensional; CT = computed tomography.

Section 7.2.5.3 Follow-up of small abdominal aortic aneurysm: Web Table 2

Web Table 2 **Pooled (meta-analysis) estimates of abdominal aortic aneurysm growth and rupture for men and women (reproduced with permission from JAMA)[365].**

	AAA Diameter, cm									
	3.0		3.5		4.0		4.5		5.0	
	Mean (95% CI)	95%PI	Mean (95% CI)	95%PI	Mean (95% CI)	95%PI	Mean (95% CI)	95%PI	Mean (95% CI)	95%PI
Growth rate, mm/y										
Men	1.28 (1.03–1.53)	0.17–2.40	1.86 (1.64–2.08)	0.85–2.88	2.44 (2.22–2.65)	1.47–3.41	3.02 (2.79–3.25)	2.00–4.04	3.61 (3.34–3.88)	2.45–4.77
Women	1.46 (1.03–1.53)	0.03–2.89	1.98 1.65–2.32	0.75–3.22	2.51 (2.22–2.81)	1.47–3.56	3.06 (2.80–3.33)	2.18–3.95	3.62 (3.36–3.89)	2.79–4.45
Time to breach surgery threshold, y[a]										
Men	7.4 (6.7–8.1)	4.9–11.3	5.0 (4.6–5.4)	3.4–7.1	3.2 (3.0–3.4)	2.3–4.4	1.8 (1.7–2.0)	1.3–2.5	0.7 (0.6–0.8)	0.4–1.2
Women	6.9 (6.1–7.8)	4.5–10.6	4.8 (4.3–5.3)	3.3–6.8	3.1 (2.9–3.4)	2.3–4.3	1.8 (1.7–2.0)	1.3–2.5	0.7 (0.6–0.8)	0.4–1.3
Rateor rupture, per 1000 person-years										
Men	0.5 (0.3–0.7)	0.3–0.7	0.9 (0.6–1.3)	0.5–1.5	1.7 (1.1–2.4)	0.6–4.3	3.2 (2.2–4.6)	1.0–10.0	6.4 (4.3–9.5)	1.7–23.5
Women	2.2 (1.3–4.0)	0.9–5.7	4.5 (2.8–7.2)	2.1–9.7	7.9 (4.5–13.9)	1.7–36.1	14.7 (8.1–27.7)	2.2–95.1	29.7 (15.9–55.4)	3.9–222.9
Time to 1% chance of rupture, y[b]										
Men	8.5 (7.0–10.5)	5.1–14.2	5.5 (4.4–6.8)	2.8–10.7	3.5 (2.8–4.3)	1.8–6.9	2.2 (1.8–2.8)	1.1–4.4	1.4 (1.2–1.8)	0.7–2.8
Women	3.5 (1.9–6.4)	0.8–14.6	2.1 (1.2–3.6)	0.4–11.1	1.4 (0.9–2.1)	0.3–5.8	0.9 (0.6–1.4)	0.2–3.5	0.7 (0.5–1.1)	0.2–3.3

Abbreviation: AAA, aortic abdominal aneurysm; PI, prediction interval.
[a]Time taken to reach a 10% chance that the 5.5-cm threshold for surgery has been crossed.
[b]Time taken to reach a 1% chance of rupture.

Section 9.1.2 Diagnosis: Web Table 3

Web Table 3 **Semi-quantitative grading of severity of aortic atherosclerosis[505,506]**

Grade	
Grade I	Normal aorta
Grade II	Increased intimal thickening without luminal irregularities
Grade III	Single or multiple protruding atheromas
Grade IV	Atheroma with mobile or ulcerated (complicated) structure

Section 10.2 Treatment: Web Table 4

Web Table 4 Inflammatory diseases associated with aortitis

Disease	Diagnostic criteria	Definitive diagnosis
Giant cell arteritis[540]	• Age at onset >50 years • Recent-onset localized headache • Temporal artery tenderness or pulse attenuation • Elevated erythrocyte sedimentation rate >50 mm/h • Artery biopsy showing necrotizing vasculitis	Three or more criteria are present (sensitivity >90%; specificity >90%)
Takayasu arteritis[525]	• Age at onset <40 years • Intermittent claudication • Diminished brachial artery pulse • Subclavian artery or carotid bruit • Systolic blood pressure variation of >10 mmHg between arms • Aortographic evidence of aorta or aortic branch stenosis	Three or more criteria are present (sensitivity 90.5%; specificity 97.8%)
Behçet disease[526]	• Oral ulceration • Recurrent genital ulceration • Uveitis or retinal vasculitis • Skin lesions, erythema nodosum, pseudofolliculitis or pathergy	Oral ulceration plus two of the other three criteria
Ankylosing spondylitis[527]	• Onset of pain at age <40 years • Back pain for >3 months • Morning stiffness • Subtle symptom onset • Improvement with exercise	Four of the diagnostic criteria are present

BP = blood pressure.